Basic

Immunity to infection

Research Article

Listeria monocytogenes induces an interferon-enhanced activation of the integrated stress response that is detrimental for resolution of infection in mice

Carolina Valderrama[1,2]*, Amy Clark*[3]*, Fumihiko Urano*[3]*, Emil R. Unanue*[1] *and Javier A. Carrero*[1] (iD)

[1] Division of Immunobiology, Department of Pathology and Immunology, Washington University School of Medicine, St. Louis, MO, USA
[2] Department of Microbiology, PhD Biomedical Sciences Program, School of Medicine, Universidad Nacional de Colombia, Bogotá, Colombia
[3] Division of Endocrinology, Metabolism and Lipid Research, Department of Medicine, Washington University School of Medicine, St. Louis, MO, USA

Type I interferons (IFNs) induce a detrimental response during *Listeria monocytogenes* (*L. monocytogenes*) infection. We were interested in identifying mechanisms linking IFN signaling to negative host responses against *L. monocytogenes* infection. Herein, we found that infection of myeloid cells with *L. monocytogenes* led to a coordinated induction of type I IFNs and activation of the integrated stress response (ISR). Infected cells did not induce *Xbp1* splicing or BiP upregulation, indicating that the unfolded protein response was not triggered. CHOP (*Ddit3*) gene expression was upregulated during the ISR activation induced by *L. monocytogenes*. Myeloid cells deficient in either type I IFN signaling or PKR activation had less upregulation of CHOP following infection. CHOP-deficient mice showed lower expression of innate immune cytokines and were more resistant than wild-type counterparts following *L. monocytogenes* infection. These findings indicate that *L. monocytogenes* infection induces type I IFNs, which activate the ISR through PKR, which contributes to a detrimental outcome in the infected host.

Keywords: CHOP · Integrated stress response · Listeriolysin O · Listeria · Mouse · Type I interferon

Additional supporting information may be found in the online version of this article at the publisher's web-site

Introduction

Listeria monocytogenes (*L. monocytogenes*) is a Gram-positive facultative intracellular pathogen responsible for listeriosis [1]. Experimental infections with *L. monocytogenes* have led to profound insights into the cell biological and immunological responses of the infected host. Listeriolysin O (LLO) is an acid-dependent pore-forming toxin [2] that is both the major virulence factor and immunogenic protein of *L. monocytogenes* [3]. LLO is required by intracellular *L. monocytogenes* to escape from the phagolysosome toward the cytosol allowing bacterial survival, replication, and cell-to-cell spread. LLO is cytotoxic, triggering programmed cell death at low nanomolar concentrations and cell lysis at higher concentrations [4, 5]. It is also responsible for inducing the death

Correspondence: Dr. Javier A. Carrero
e-mail: jacarrer@wustl.edu

of *L. monocytogenes* infected cells [6]. LLO induces multiple cellular changes, which include loss of membrane integrity [7], mobilization of intracellular calcium storage [8], autophagy [9], and apoptosis [10, 11]. Our laboratory has been interested in the cellular death and early innate response to *L. monocytogenes* infection, with a focus on LLO and type I interferon (IFN). This work led us to examine the role of the unfolded protein response (UPR) and integrated stress response (ISR) in *L. monocytogenes* pathogenesis.

The canonical response to endoplasmic reticulum (ER) stress is the result of a complex integrated signaling transduction pathway known as the UPR. The UPR stress sensors ATF6, PERK, and IRE1α transduce information about the folding status of the ER to the cytosol and nucleus in order to restore protein-folding capacity. Depending on the time and strength of the stimulus, the UPR either restores homeostasis or induces programmed cell death [12, 13]. The UPR is activated by a variety of cellular insults that include microbes and their proinflammatory products. Viral infections with dengue fever virus [14], hepatitis C [15–17], influenza A [18], and lymphocytic choriomeningitis virus [19] trigger the UPR. Infections with the parasite *T. gondii* [20], and the bacteria Pseudomonas *aeruginosa*, [21] and *M. tuberculosis* [22] also trigger UPR. So do microbial products such as LPS [23, 24] and cholera toxin [25]. Nevertheless, the mechanisms leading to activation of the UPR pathways and its role under in vivo infection remain incompletely defined. The UPR may affect a number of cellular responses such as calcium homeostasis, lipid metabolism, redox state, protein glycosylation, and autophagy [26]. The detailed relationship between the different UPR responses and the specific cellular processes that drive inflammation is an emerging field.

The kinase PERK can autoactivate in response to perturbations of the ER such as the presence of unfolded proteins, i.e. the UPR. Activated PERK phosphorylates and inactivates the eukaryotic translation-initiation factor 2α (eIF2α) [27]. Phosphorylation of eIF2α negatively affects translation in a dosage-dependent manner, but it leads to the translation of the cap-independent transcription factor ATF4 [28, 29]. ATF4 triggers the transcription of the proapoptotic transcription factor CHOP (*Ddit3*) and the phosphatase regulatory protein GADD34 (*Ppp1r15a*) [30]. There are two general outcomes of PERK activation: (i) low level of activation leads to reduction in ER protein load, dephosphorylation of P-eIF2α, and cellular survival and (2) high level of CHOP expression leads to death of the affected cell (12). Besides PERK, other cytosolic kinases can also phosphorylate eIF2α. For example, the hem-regulated inhibitor kinase (HRI; involved in erythropoiesis), the general control nonderepressible-2 (GCN2; senses amino acid starvation), and the IFN-induced double-stranded RNA-activated protein kinase (PKR; senses infections) are all eIF2α kinases [31]. The term ISR is used to refer to the pathway of eIF2α-mediated stress that is triggered by any of the eIF2α kinases [32].

The main mode of PKR activation is through binding of virally derived dsRNA to its N-terminal dsRNA binding domain and subsequent autophosphorylation. Two additional mechanisms of PKR activation have been proposed recently: the formation of endogenous microRNA-derived dsRNAs and protein ISGylation [33, 34]. Both mechanisms can be triggered by type I IFN signaling

pathways. Type I IFNs induce the expression of PKR and high concentrations of PKR transcripts have been proposed as an endogenous source of dsRNA [33]. High concentrations of PKR protein allow it to homodimerize and autophosphorylate in the absence of dsRNA [34]. Furthermore, type I IFNs trigger the expression of ISG15, an activator of PKR in the absence of viral infections [34]. ISG15 modifies the lysine residues at positions 69 and 159 of PKR allowing its dimerization and autophosphorylation [34].

During *L. monocytogenes* infection, type I IFNs induce a detrimental response in the host that includes apoptosis of lymphocytes and myeloid cells, and the secretion of immunosuppresive cytokines, such as IL-10 [35]. Mice deficient in the type I IFN receptor (IFNAR KO) are resistant to *L. monocytogenes* infection [36–38]. *Listeria monocytogenes* invades the cytosol in an LLO-dependent manner and this biological activity is required for the induction of type I IFNs [39, 40]. These findings led us to hypothesize that either the presence of cytosolic bacteria or LLO could trigger cellular stress mechanisms. For this reason, we examined whether cells infected with *L. monocytogenes* or treated with LLO protein developed a UPR or ISR. Both infection and LLO treatment increased the expression of the transcription factor *Ddit3* (CHOP), as well as other markers of the PERK pathway. PERK was activated early after *L. monocytogenes* infection, and its downstream signaling was amplified by type I IFN, all in the absence of detectable activity by other two members of the UPR. We found that induction of type I IFN by *L. monocytogenes* infection led to PKR activation, which in turn enhanced the PERK pathway-associated response. Our results suggest that *L. monocytogenes* activated the ISR. The biological consequence of ISR activation was examined in *Ddit3*−/− (CHOPKO) mice that showed increased resistance to *L. monocytogenes* infection. We suggest that induction of ISR is as a novel mechanism that helps to explain the detrimental response of the host to type I IFN signaling during *L. monocytogenes* infection.

Results

Listeria monocytogenes infection triggers the ISR

To determine if *L. monocytogenes* infection induces ER stress in APCs, we evaluated mRNA expression levels of canonical ER stress markers [47]. These markers allowed the identification of which pathway(s) of the UPR were activated. To assess general activation of the UPR, we measured the ER chaperones BIP (*Hspa5*) and *Wfs1* [48, 49]. For monitoring IRE1α activation, we measured *Xbp1* spliced-form (*Xbp1s*) levels [50]. To measure PERK pathway activation, we evaluated CHOP (*Ddit3*) expression levels [13]. We evaluated two strains of *L. monocytogenes,* a wild-type (WT) strain that secretes listeriolysin (LLO) (LM LLO) and another that does not secrete LLO, the Δ*hly* (LM ΔLLO mutant). As a positive control for the induction of ER stress, we used the sarco/endoplasmic reticulum Ca2+ ATPase (SERCA) inhibitor thapsigargin (TG). Two APCs were used: GM-CSF-derived bone marrow dendritic cells (BMDC) or M-CSF-derived bone marrow macrophages (BMM).
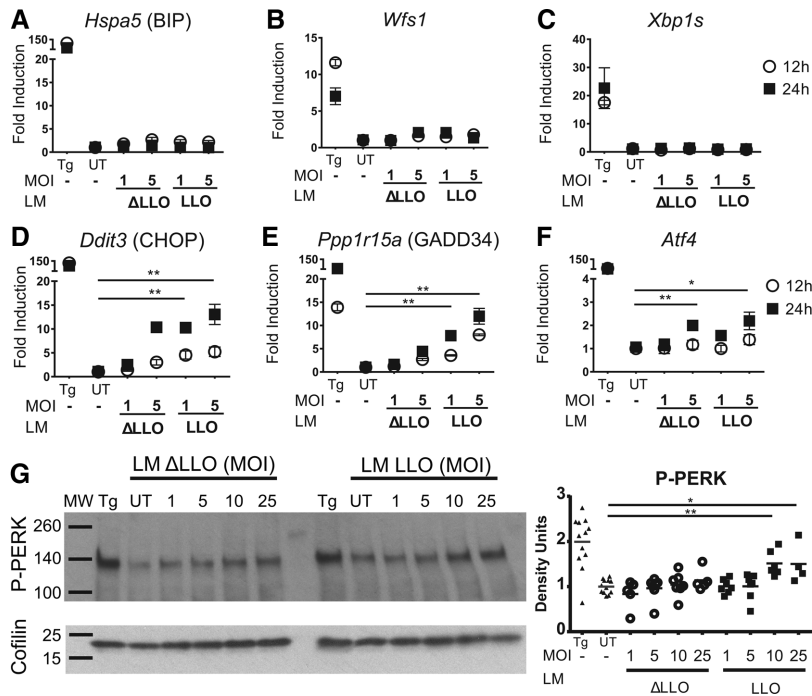
Figure 1. The ISR is triggered in BMDCs infected with *L. monocytogenes*. A–C. C57BL/6 BMDCs were infected with two different strains of *L. monocytogenes*, WT *L. monocytogenes* (LM LLO) and *L. monocytogenes* Δ*hly* that lack LLO secretion (LM ΔLLO). Two different MOIs were tested. After infection, BMDCs were incubated with indicated *L. monocytogenes* strain for 12 or 24 h. cDNA was synthesized from extracted mRNA and gene expression measured by qRT-PCR. (A) *Hspa5* (BIP); (B) *Wfs1*; (C) *Xbp1s*; (D) *Ddit3* (CHOP); (E) *Ppp1r15a* (GADD34); and (F) *Atf4* were amplified with specific primers by qRT-PCR. The fold change in gene expression was calculated using $2^{-\Delta\Delta CT}$, where $\Delta\Delta C_T = (C_{T,\,Target} - C_{T,\,Actin})_{Treated\,x} - (mean\,C_{T,\,Target} - mean\,C_{T,\,Actin})_{Untreated}$. TG was used as a positive control. Symbols represent mean ± SEM. Results are pooled from two independent experiments performed in triplicates. (G) C57BL/6 BMDCs were infected with *L. monocytogenes* with the indicated MOIs. The two strains of *L. monocytogenes* were tested. Whole cell extracts were analyzed by western blot for phosphorylated-PERK (P-PERK) and Cofilin as a loading control. Mean of densitometric quantification is plotted. Symbols represent densitometry on 4–12 biological replicates performed in six independent experiments. MW, molecular weight; UT, untreated condition. Thapsigargin (TG) was used as a positive control. *p* value was calculated with Mann–Whitney test *$p < 0.05$, **$p < 0.001$.

Listeria monocytogenes infection of BMDC induced less than a twofold upregulation in *Hspa5* and *Wfs1* expression relative to the untreated condition (Fig. 1A and B). *Xbp1* splicing was not detected (Fig. 1C). These findings indicate that the complete canonical UPR pathway was not induced following infection with *L. monocytogenes*. *Listeria monocytogenes* infection induced an ~10- to 15-fold upregulation in the expression of *Ddit3* (CHOP) (Fig. 1D) that was time and bacterial load dependent. It has been shown that *Ddit3* expression is upregulated by the phosphorylation of eIF2α by PERK and other members of the eIF2α kinase family of enzymes, including, PKR, GCN2, and HRI (12-13). PERK pathway activation was confirmed by the finding of an eightfold increase in the expression of the CHOP-inducible gene *Ppp1r15a* (GADD34) (Fig. 1E). *Ddit3* upregulation was also observed with high multiplicity of infection (MOI) of the Δ*hly L. monocytogenes* strain. After 24 h of infection, *Ddit3* expression increased ~10-fold in BMDC relative to the untreated cells (Fig. 1D). Other downstream ISR markers were also upregulated: ~5-fold for *Ppp1r15a* and ~2-fold for *Atf4* (Fig. 1E and F). Similar results were seen in BMM (Supporting Information Fig. 1). We also found that PERK phosphorylation increased with higher bacterial loads of WT *L. monocytogenes* as early as 3 h of in vitro infection in BMDC (Fig. 1G). Finally, we also detected protein-level induction of ATF4, as infection of BMM and BMDC allowed for its detection, as assayed by immunoblotting (Supporting Information Fig. 2A and B). *Listeria monocytogenes* infection selectively triggered the PERK pathway in APCs in the absence of the canonical ER stress response. Therefore, we concluded *L. monocytogenes* triggered the ISR.

This finding led us to evaluate phagocytosis as a possible triggering factor of the ISR activation. Uptake of latex beads by BMDC did not induce an increase in *Ddit3* expression (Supporting Information Fig. 2C). We concluded that endocytosis was not sufficient to trigger CHOP. Therefore, in addition to LLO, other *L. monocytogenes* virulence factors or pathogen-associated molecular patterns must be involved in early ISR activation.

LLO induces the ISR

To evaluate the direct effect of LLO in the ISR activation in the absence of other *L. monocytogenes* inflammatory molecules, we pulsed BMDCs with WT recombinant LLO (LLOWT) [46]. We used concentrations previously established to be nonlethal to myeloid cells [4, 10, 11]. After treatment with LLO, the ISR was activated (Fig. 2A–C). Expression of *Ddit3* increased sixfold and *Ppp1r15a* increased twofold relative to the untreated condition. We did not find significant changes in *Hspa5* or *Wsf1* expression, and *Xbp1* splicing was not detected (Fig. 2D–F). We also tested a mutant variant of LLO, LLOLT, that lacks the hemolytic activity of LLOWT and that allowed us to test it at 10 and 100-times higher concentrations. LLOLT differs from LLOWT only in an amino acid inversion T515L-L516T [51]. LLOLT triggered the ISR with an upregulation of *Ddit3* of ~20-fold, *Pppr15a1* of ~10-fold, and *Atf4* of ~10-fold (Fig. 2G–I). At higher concentration, we detected upregulation of ~2-fold for *Hspa5*, ~2-fold for *Wsf1*, and ~2-fold for *Xbp1s* (Fig. 2J–L). Thus, LLO protein triggered the ISR unrelated to its cytolytic activity.

To exclude an LPS contamination in our LLO preparations as a confounding trigger of the ISR, we measured *Ddit3* expression induced by LLOWT in the presence of the LPS-binding compound polymixin B (PMB) (Supporting Information Fig. 2D). Purified LPS induced a ~20-fold increase in expression of *Ddit3* and this response was abolished by pretreatment of the LPS with PMB. LLOWT upregulation of *Ddit3* was unaffected by the presence
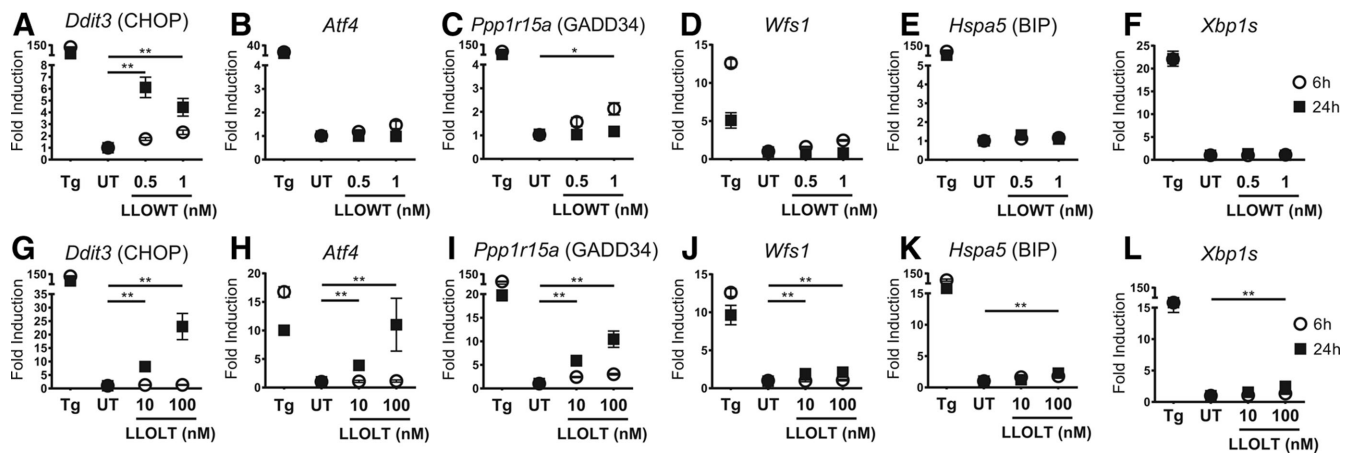
Figure 2. The ISR is triggered by recombinant LLO protein. To avoid cell death, C57BL/6 BMDCs were pulsed with low concentrations of recombinant WT LLO protein (LLOWT) (**A–F**) or high concentrations of a nonlytic LLO mutant protein (LLOLT) (**G–L**) and incubated with indicated strains 6 and 24 h. cDNA was synthesized from extracted mRNA and gene expression measured by qRT-PCR. (**A, G**) *Ddit3* (CHOP); (**B, H**). *Atf4*; (**C, I**) *Ppp1r15a* (GADD34); (**D, J**). *Wfs1*; (**E, K**) *Hspa5* (BIP); (**F, L**) *Xbp1s* were amplified with specific primers by qRT-PCR. The fold change in gene expression was calculated using $2^{-\Delta\Delta CT}$. Dots are mean ± SEM of six biological replicates. UT, untreated condition; TG was used as a positive control. *p* value was calculated with Mann–Whitney test *$p < 0.05$, **$p < 0.001$. Results are pooled from two independent experiments performed in triplicates.

of PMB. Therefore, the increase in CHOP expression induced by LLOWT was not a result of LPS contamination.

Listeria monocytogenes induced activation of the ISR leads to inflammatory cytokine gene expression

To establish whether the ISR activation played a role in the cytokine response induced by *L. monocytogenes* infection, we examined BMDC and BMM from *Ddit3*$^{-/-}$ mice (CHOP KO). We tested the CHOP-deficient APCs to avoid the aberrations in ER morphology and physiology described in PERK-deficient cells [52], and the hematopoietic system abnormalities in ATF4 KO mice [53]. We measured the expression of the type I IFNs (Pan-Ifna and *Ifnb1*), IL-12α (*Il12a*), IL-12β (*Il12b*), and IL-1β (*Il1b*) following infection of CHOP KO BMDC and BMM. In general, we found decreased expression of inflammatory cytokine genes in BMDC and BMM from CHOP KO compared to cells from normal mice, with the exception for *Il12* that increased only in BMDC (Fig. 3). The overall cytokine responses peaked at 12 h of infection in WT APC and decreased by 24 h. After 12 h, expression levels of *Il12a*, *Il12b*, and *Il1b*, were ∼200-fold, ∼3500-fold, and ∼1500-fold higher in controls versus CHOP KO BMDC (Fig. 3A). For *Il12b* and *Il1b* expression changes were detectable even after 24 h. There was induction of IFN-α and IFN-β gene expression at the 12 h time. This response was reduced by 1/2 or 1/3 in the BMDC from CHOP KO mice. Also to note is that LM ΔLLO triggered IFN gene expression but required higher MOI compared to WT *L. monocytogenes*. CHOP KO BMM also showed a statistically significant decrease of *Ifna*, *Ifnb1*, and *Il1b* (Fig. 3B). We concluded that ISR activation regulated the innate immune cytokine induction of APCs following *L. monocytogenes* infection.

We also evaluated the expression of other ER stress-related genes in CHOP KO APCs after infection (Supporting Informa-

tion Fig. 3). We found less than twofold change in expression of *Hspa5* and *Wfs1* in both BMDC and BMM. Additionally, *Pppr15a1* was decreased to half its normal level of expression in BMDC (Supporting Information Fig. 3A). Thus, the impairment of the PERK pathway in CHOP KO APCs did not trigger other compensatory ER stress responses following *L. monocytogenes* infection.

Type I IFN acting through PKR enhances *L. monocytogenes* activation of the ISR

Listeria monocytogenes invades the cytosol and initiates a type I IFN response [54]. One outcome of type I IFN receptor signaling is the activation of PKR, which in turn induces activation of the ISR, in addition to PERK phosphorylation [32]. Hence, we hypothesized that we may have a feed-forward transcription loop in which type I IFN acting through PKR activates the ISR that enhances PERK-associated signaling following *L. monocytogenes* infection.

We evaluated the expression of *Ddit3* (CHOP) as a marker of the ISR activation. In APCs derived from mice deficient in the type I IFN receptor (IFNAR KO), *Ddit3* transcription was decreased significantly when compared to WT controls (Fig. 4A and B). Blockade of PKR activation using the chemical inhibitor C16 also led to a significant inhibition of the ISR activation at 12 h (Fig. 4A and B) [55, 56]. The effect of C16 was not seen at 24 h postinfection in BMM suggesting that the effect of the inhibitor was not absolute or was reversible.

Human PKR has been better characterized than mouse PKR. Based on its DNA sequence the molecular mass is about 62 kDa, meanwhile, in the mouse it is 59 kDa. Human PKR has 14 phosphorylation sites, among them, the residue T451 (p-T451) is required to generate an active kinase. This corresponds p-T414 of mouse PKR. Conventional western blotting techniques made to identify active PKR (p-T451) detect diverse molecular weights of PKR in a
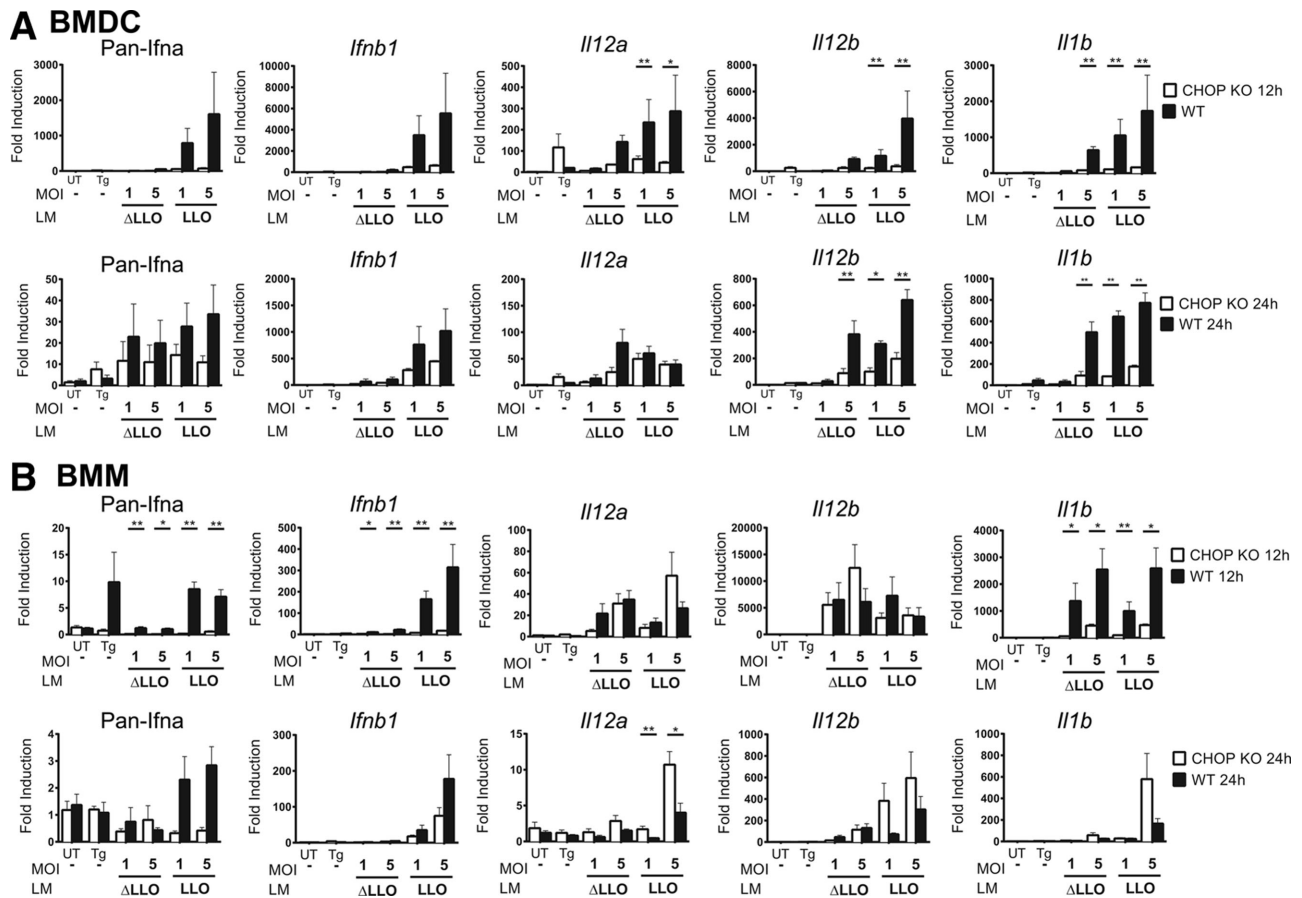
Figure 3. The role of the ISR impairment in innate immune cytokines response from *L. monocytogenes* infected APC. C57BL/6 and PERK pathway impaired, CHOP knockout mice (CHOP KO) BMDC or BMM were infected with WT *L. monocytogenes* (LM LLO) and *L. monocytogenes* Δ*hly* (LM ΔLLO). Two different MOIs were tested. (**A**) BMDCs or (**B**) BMMs were incubated with indicated *L. monocytogenes* strains for 12 and 24 h. cDNA was synthesized from extracted mRNA. Then specific primers were used to amplify Pan-Ifna; Ifn-β; Il-12α; Il-12β; and Il-1β by qRT-PCR. The fold change in gene expression was calculated using $2^{-\Delta\Delta CT}$. Bars are mean ± SEM of six biological replicates. UT, untreated condition; Tg, thapsigargin 0.1 μM as a positive control. *p*-value was calculated with Mann–Whitney test $*p < 0.05$, $**p < 0.001$. Results are pooled from two independent experiments performed in triplicates.

range of 50–75 kDa [57]. Cytoplasmic and nuclear PKR forms also have multiple isoelectric points due to different phosphorylation states. PKR also has diverse posttranslational modifications. There is no monoclonal antibody available for mouse p-PKR detection and the available regents have been made for human PKR, which cross-react with mouse PKR. Recent studies showed that human PKR mRNA has no alternate splicing products [57]. Furthermore, upregulation of PKR activity evaluated by kinase assays in mouse models is also accompanied with an increase in PKR protein and mRNA levels [58]. This is consistent with the reported autoregulation of PKR expression upon stimulation of its activity [59]. For these reasons, we measured *Eif2ak2* (the PKR gene) transcription as a marker of PKR activation and found ∼3-fold increase in its expression of following *L. monocytogenes* infection of both BMDC and BMM (Fig. 4C and D). Additionally, treatment of APCs with the PKR inhibitor C16 prevented more than 50% the upregulation of *Eif2ak2* expression detected after infection. (In BMDC, PKR inhibition was detected up to 24 h postinfection. In BMM, PKR inhibition was found at 12 h but not 24 h postinfection.) There-

fore, we concluded that *L. monocytogenes* infection enhances the ISR activation through PKR phosphorylation triggered by type I IFN receptor signaling.

BMM and BMDC were treated with 1 μM GSK2656157 for 1 h and then infected with *L. monocytogenes* or treated with TG. At this dosage, GSK2656157 is reported to inhibit phosphorylation of eIF2α, and protein expression of ATF4 and CHOP downstream of both tunicamycin and TG treatment, while maintaining PKR activity.

We evaluated ISR induction at 12 and 24 h postinfection. As in the rest of the manuscript, we used TG as a positive control for the induction of ISR and as a benchmark for the inhibitory effects of GSK2656157. In the TG-treated cells, the PERK inhibitor reduced the expression of *Ddit3* (CHOP), albeit not completely (Supporting Information Fig. 4). This result confirmed that our dosage and treatment times for GSK2656157 were able to reduce PERK-induced *Ddit3* expression.

The PERK inhibitor led to an increase in the upregulation of the level of *Ddit3* expression following *L. monocytogenes* infection.
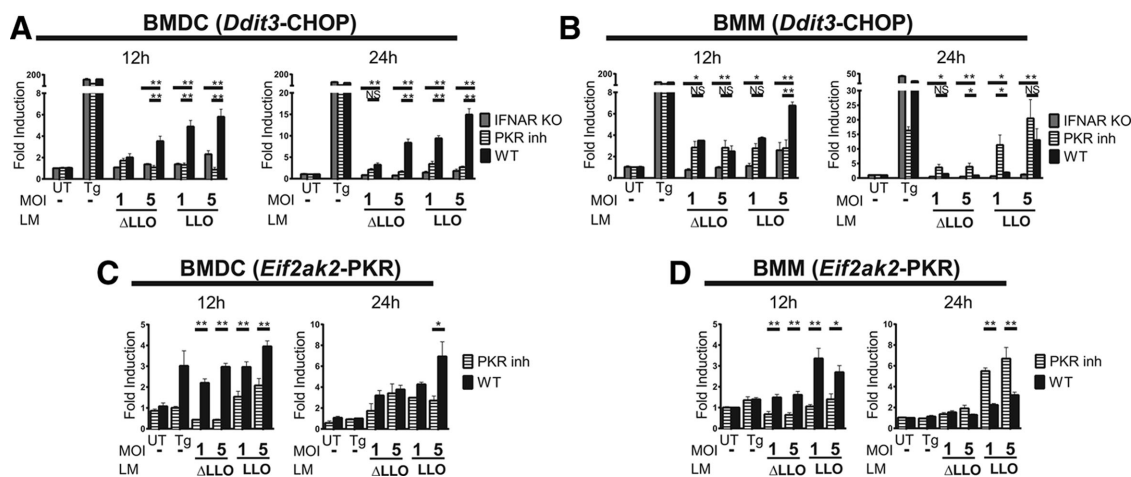
Figure 4. Type I IFN triggers the ISR through PKR activation. (A) BMDCs or (B) BMMs from CHOP KO, IFNAR KO, C57BL/6 mice, and WT APCs in which PKR phosphorylation was inhibited with C16 (PKR inh) were infected with WT *L. monocytogenes* (LM LLO) and *L. monocytogenes* Δ*hly* (LM ΔLLO) for 12 and 24 h. Two different MOIs where tested. cDNA was synthesized from extracted mRNA. Then specific primers were used to amplify CHOP (*Ddit3*) by qRT-PCR. (C) BMDCs or (D) BMMs were incubated with or without the PKR phosphorylation inhibitor C16 at 2 μM and infected with LM LLO and LM ΔLLO. Then specific primers were used to amplify *Eif2ak2* (PKR) by qRT-PCR. The fold change in gene expression was calculated using $2^{-\Delta\Delta CT}$. Bars are mean ± SEM of six biological replicates. UT, untreated condition. TG was used as a positive control. *p*-value was calculated with Mann–Whitney test *$p < 0.05$, **$p < 0.001$. Results are pooled from two independent experiments performed in triplicates.

We attribute the paradoxical *Ddit3* upregulation induced by PERK inhibition during *L. monocytogenes* infection to NRF2/Keap1 pathway inhibition. NRF2/Keap1 pathway is activated by PERK and antagonizes the expression of *Ddit3*. Thus, when PERK is blocked, but PKR is still active, the ISR response prevails and *Ddit3* (CHOP) is upregulated

The ISR activation modulates host handling of *L. monocytogenes* infection

To establish the role of the ISR activation during *L. monocytogenes* infection *in vivo*, we examined C57BL/6 CHOP KO mice during the early phase of the infection. We infected CHOP KO and WT mice with *L. monocytogenes* and followed them for survival (Fig. 5A). At an LD_{50}, 60% of WT mice in contrast to 17% of CHOP KO mice died within the first 10 days of infection. CHOP KO mice displayed an average of ten times lower bacterial burden in spleens and livers than WT mice at day 3 postinfection (Fig. 5B).

CHOP KO mice contained, on average, no detectable bacterial burden in their spleens and livers at day 7 postinfection (Fig. 5C). In contrast, WT mice still had a detectable burden in livers at day 7. The differences in bacterial burden were reflected in the tissue pathology. The extensive splenic white pulp apoptosis and necrosis reported in the WT mice during the first 72 h of infection was reduced in the CHOP KO mice [35] (Fig. 5D). The number and size of liver microabscesses was also decreased in CHOP KO mice (Fig. 5E). Finally, CHOP KO mice showed lower innate immune cytokine levels in serum than WT mice (Fig. 5F–H), similar to what was shown in CHOP KO BMDC and BMM (see above). At 24 h after infection, we found statistically significant decrease in IFN-γ, IL-6, and MCP-1 production in CHOP KO versus WT mice. [We detected no difference in TNF-α production following *L. mono-*

cytogenes infection of WT versus CHOP KO macrophages in vitro or mice in vivo (Supporting Information Fig. 5).] Together our findings show that CHOP KO mice are more resistant to *L. monocytogenes* infection than WT mice. Thus, we concluded that the ISR activation is detrimental to host handling of *L. monocytogenes* infection.

Discussion

Our results identify a novel and important mechanism that explains part of the detrimental response induced by type I IFN during *L. monocytogenes* infection. We show that *L. monocytogenes* triggers the ISR and the main component of this response is driven by type I IFN signaling. Type I IFN induces a feed-forward transcription loop, the consequence of which is the activation of CHOP resulting in further IFN production as surmised by the effects of CHOP KO cells. The ISR activation is detrimental to *L. monocytogenes* infected mice leading to increased morbidity and mortality.

Our findings indicate that PKR is one of the cytosolic enhancers of the ISR during *L. monocytogenes* infection. Although high MOI of *L. monocytogenes* infection trigger phosphorylation of PERK as early as 3 h, a second signal is required to maintain and/or enhance the ISR in infected cells at lower doses. PKR acts as a link between the ISR activation and type I IFN response. Indeed, cells from the IFNAR KO mice had markedly decreased transcription of PKR. It is known that type I IFN induces PKR activation increasing its synthesis and autophosphorylation [34, 59]. When we inhibited PKR phosphorylation, *Ddit3* expression was decreased. The whole mechanism for activation suggests that the release of type I IFN after *L. monocytogenes* internalization activates PKR to phosphorylate eIF2α triggering ATF4-CHOP transcriptional program.
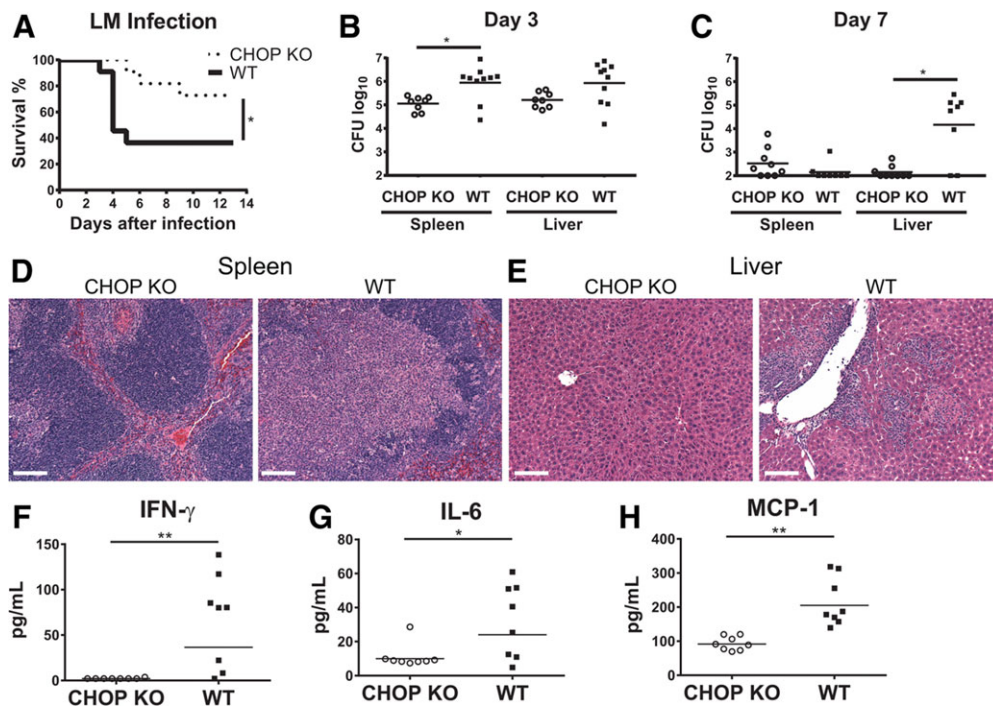
Figure 5. Impairing the ISR silencing CHOP transcription factor protects against *L. monocytogenes* infection in vivo. C57BL/6 and CHOP KO mice were infected WT *L. monocytogenes*. (**A**) For survival assay C57BL/6 ($n = 30$ mice) and CHOP KO ($n = 20$ mice) were followed for 13 days. p value was calculated with log-rank (Mantel–Cox) test **$p < 0.005$. (**A–D**) For colony counts in spleens and livers, mice were sacrificed after (**B**) 3 days ($n = 10$ WT, $n = 8$ CHOP KO mice) and (**C**) 7 days ($n = 8$ WT, $n = 9$ CHOP KO mice). For histological evaluation mice were infected with 10^4 CFU (**D**) spleens and (**E**) livers from infected mice at day 3 were isolated, fixed, and stained with H&E. Magnification 10×. Scale bar represents 100 µm. Pictures are representative of $n = 4$ WT and $n = 4$ CHOP KO mice. (F–G) For serum cytokines evaluation, mice were infected with 10^4 CFU, $n = 8$ mice per group. (F) IFN-γ, (G) IL-6, and (H) MCP-1 were quantified by CBA after 24 h. Dots represent biological replicates and the mean of each condition is plotted. Data are pooled from two to three independent experiments with four to ten mice per experiment. p-value was calculated with Mann–Whitney test *$p < 0.05$, **$p < 0.001$.

Our results showed that *L. monocytogenes* triggers PERK phosphorylation 3 h after infection, before the transcriptional markers are activated. PERK phosphorylation not only triggers a cell death program but also is an autoregulated pathway that allows cell survival [13, 60]. The survival branch described as part of the PERK pathway is an ISR-independent response that is also triggered by p-PERK, which directly activates NRF2/Keap1 pathway and elicits an antioxidant program [61]. Both pathways share ATF4 activation but NRF2/Keap1 pathway inhibits CHOP expression. Thus, we speculate that *L. monocytogenes* could activate both PERK pathway branches. In the presence of CHOP, as part of the ISR, PERK-eIF2α-CHOP branch predominates sending the cell to oxidative stress and death [62, 63]. In the absence of CHOP, as is the case of CHOP KO mice, the PERK-NRF2-Keap1 activation could be promoting cell survival in the same way as previously described for CHOP inhibition in a cecum-ligation induced sepsis model [64]. We also found that a specific p-PERK inhibitor [65] is able to inhibit both pathways but when PKR is still active, the ISR response prevails and *Ddit3* (CHOP) is upregulated in APC. Future studies will be required to clarify the cross-talk between both PERK pathway branches and the mechanism of this early PERK phosphorylation induced by *L. monocytogenes*.

Ddit3 (CHOP) has been reported as highly upregulated gene after *L. monocytogenes* infection [39], but its role as a component of

the ISR and its association with type I IFN signature response was unknown. Here, we found that *L. monocytogenes* infection induced upregulation of *Atf4*, *Ddit3* (CHOP), and *Ppp1r15a* (GADD34). Accordingly, we confirmed the ISR activation by *L. monocytogenes* infection as a result of Type I IFN signaling. Also, the absence of increased expression of other ER stress markers, such as *Hspa5* (BIP), *Wfs1*, and spliced *Xbp1s* (XBP1s), allowed us to exclude this PERK pathway activation as part of the canonical UPR. Previous studies showed that low MOI of *L. monocytogenes* induce XBP1s at 8 h [23]. In contrast, our model of infection tested 10–50 times higher MOIs in later time points 12 and 24 h. XBP1s has been proposed as an early adaptive response to stressors [13]. Based on both findings, we suggest that at low bacterial MOIs the adaptive cellular response dominates. Meanwhile, at high MOIs and after long infection times the adaptive response is not sustained and the cell death fate triggered by the ISR predominates.

CHOP is one of the major effector transcription factors of the ISR. CHOP induces a number of effects such as oxidative stress [62], ER-calcium release [66], inflammasome activation [67], proinflammatory cytokines secretion [68], and cell death [63, 69, 70]. *Listeria monocytogenes* is a well-known inductor of different forms of cell death including apoptosis [35] and pyroptosis [71]. On the other hand, CHOP KO mice have decreased apoptotic phenotypes [66, 72]. In this study, we found CHOP KO

mice infected with *L. monocytogenes* had a decrease in splenic cell death, fewer liver microabscesses, decreased bacterial proliferation, and a better survival than WT mice. Additionally, CHOP KO mice had a reduced release of systemic inflammatory cytokines. We also confirmed lower expression of inflammatory cytokines in both BMDC and BMM from CHOP KO mice, with the exception for IL12 that increased in CHOP KO BMM [38]. Together our findings suggest that in the absence of CHOP, the earliest DCs and macrophages that phagocytose the bacteria may be more resistant to cell death. Consequently, the local control of the infection at early steps, when DCs and macrophages are viable, leads to an immune response that avoids a strong proinflammatory cytokine release and the recruitment of more immune cells. As a result, tissue damage in spleen and liver was decreased.

In summary, we described an alternative pathway that allows a better understanding of the detrimental response induced by type I IFN release during *L. monocytogenes* infection, the ISR activation. The specific role of the ISR in the pathogenesis of other bacterial infections remained unexplored. However, there is evidence that *M. tuberculosis* activates PERK-pathway markers and IRE1α in macrophage rich granulomas [22]. Also, homoserine lactone (HSL-C12), a membrane permeant molecule secreted by *P. aeruginosa*, is able to trigger an inflammatory response through activation of PERK pathway [21]. Based on the benign phenotype of CHOP KO mice, this study opens the possibility of exploring the use of CHOP inhibitors as an alternative or a coadjuvant to antibiotic therapies, either to enhance host responses during bacterial infections, or to decrease the extensive organ damage associated with antibacterial immune responses.

Materials and methods

Mice

WT C57BL/6 and C57BL/6 CHOP knock out (B6.129S(Cg)-Ddit3$^{tm2.1Dron}$/J) mice were purchased from Jackson Laboratory (Bar Harbor, ME). The CHOP KO mouse was made in 129S6/SvEvTac-derived W4 embryonic stem cells. The resulting mice were backcrossed and are on a mixed C57BL/6J-C57BL/6N background. After backcrossing, by single nucleotide polymorphism analysis only one marker of 32 was found to be derived from 129S6 (Jackson Laboratory). C57BL/6 IFN-αβR knock out (IFNAR KO) were obtained from Dr. Robert Schreiber (Washington University School of Medicine, St. Louis, MO). All the experiments were performed with sex and age matched mice at 8–20 weeks of age. Mice were maintained in our specific pathogen-free animal facility according to institutional guidelines and protocols approved by the Division of Comparative Medicine of Washington University School of Medicine (Association for Assessment and Accreditation of Laboratory Animal Care [AAALAC] accreditation number A3381-01). All mice were bred and maintained in the same room and on the same rack within our facility. Only mice bred in our facility were used for all of the experiments reported herein.

Cell cultures

DCs were derived from BMDC as previously described with modifications [41]. BM cells were cultured at 10^6 cells per well in 6-well plates for 6 days in GM-CSF–containing medium (pyrogen-free DMEM [Gibco, Thermo-Fisher, Waltham, MA] with 20 UI/mL GM-CSF from conditioned supernatants, 10% FCS [Hyclone, GE Healthcare, Logan, UT], 1× nonessential aminoacids [Gibco], 1 mM Na pyruvate [Gibco], 1× GlutaMAX^{TM} [Gibco], 50μM β-ME [Fluka, Sigma-Aldrich, St. Louis, MO], and kanamycin 0.1 mg/mL [Gibco]). Cultures media was replaced on day 4 with conditioned media without antibiotic.

Macrophages were derived from BMM as previously described with modifications [42]. BM cells were cultured at 10–15 × 10^6 cells in 150 mm Petri dishes for 7 days in M-CSF–containing medium (pyrogen-free DMEM with 20% L-cell conditioned media, 10% FCS, 5% Horse serum [Sigma], 1 mM Na pyruvate, 1.5 mM L-glutamine [Corning, Corning, NY], 1× penicillin/streptomycin [Gibco]). BMM were harvested on day 7 and replated at 10^6 cells per well in 6-well plates in conditioned media without antibiotic.

Listeria monocytogenes infection

Infections were performed as previously described [43]. *We used L. monocytogenes* strain EGD (LM LLO) and LM ΔLLO strain EJL1. For histological examination, small samples of spleens and livers were fixed in 10% formalin and stained with hematoxylin and eosin (H&E). Cytokines assays were performed on sera of infected mice by cytometric bead array (CBA, BD Biosciences, San Jose, CA) analysis. Mouse Inflammation Kit (BD Biosciences) was followed according to the manufacturer's instructions. CBA data were analyzed on a FACSCalibur^{TM} with CELLQuest^{TM} software and the CBA analysis software package.

For cell cultures infection, BMDC or BMM were infected for 3 to 24 h. In brief, *L. monocytogenes* strains were grown overnight on Brain-Heart-Infusion broth at 37°C. Bacteria concentration was estimated with OD$_{560}$ then indicated bacterial dilutions were made in D10F (DMEM with 10%FCS) or D10F plus the Imidazolo-oxindole PKR inhibitor C16 (Sigma). Half of the initial cells culture volume was replaced with bacteria-containing media and centrifuged at 2000 rpm per 10 min. Plates were incubated at 37°C for 30 min. Finally, cell cultures were replaced with D10F or D10F-C16 plus gentamicin at 5 μg/mL [Gibco] to kill non-phagocytized bacteria.

RNA isolation and real-time PCR

For infected BMDC and BMM, total RNA was isolated with Ambion RNAqueous-Micro Kit (Life Technologies, Carslbad, CA) following

manufacturer's instructions. RNA was quantified by OD_{260} using Nanodrop (Thermo Fisher Scientific). cDNA was obtained from total RNA using First Strand Synthesis Protocol with Reverse Transcriptase (New England BioLabs). TaqMan PCR was performed using TaqMan Fast Universal PCR Master Mix. Primers for quantitative RT-PCR were designed using the PrimeTime predesigned qPCR assays (IDT DNA, Coralville, IA), except for Pan-Ifna, which transcripts were made based on previous work [44]. PrimeTime primers employed 5'-nuclease detection. *Xbp1s* was performed using SYBR® green detection technology. To amplify the spliced form of mouse XBP-1, we used mXBP1.7S: CAG CAC TCA GAC TAT GTG CA and mXBP1.10AS: GTC CAT GGG AAG ATG TTC TGG as previously described [45]. StepOne 2.1 software was used to perform quality control and the relative expression quantification.

Recombinant LLOWT and LLOLT purification

The expression vector pET29b containing His-tagged LLO sequence (LLOWT) was provided by Dr. Daniel Portnoy (University of California, Berkeley, CA). LLOWT was purified as previously described using Ni-NTA Sepharose (Qiagen, Valencia, CA) and dialyzed extensively against storage buffer (50 mM phosphate/acetate [pH 6.0], 1 M NaCl, 1 mM EDTA, and 5 mM DTT) [10, 46]. For LLOLT, LLOWT was modified with an inversion T515L-L516T using Quickchange Site-Directed Mutagenesis kit (Agilent Technologies, Santa Clara, CA) following the manufacturer's protocol. Mutagenesis was confirmed by sequencing of constructs at the Washington University Nucleic Acids Core facility. Proteins purity was confirmed by SDS-PAGE.

Western blots

Infected BMDCs were lysed on ice in $1\times$ Laemmli buffer (for P-PERK), with Complete Protease Inhibitor Cocktail (Roche Diagnostic Systems, Indianapolis, IN), and PhosStop Phosphatase Inhibitor Cocktail (Roche Diagnostic Systems). Lysates were resolved on a 4–15% Mini-PROTEAN® TGX™ precast polyacrylamide gel (Bio-Rad) and transferred to a PVDF membrane. Rabbit mAb Phospo-PERK (Thr980) (16F8), Cofilin (D3F9) XP™ and the secondary Ab Goat anti-rabbit-HRP were purchased from Cell Signaling Technologies (Beverley, MA).

Statistical analysis

Mann–Whitney U test was used to determine significant differences between samples. All data were plotted using GraphPad Prism 6 (GraphPad Software, La Jolla, CA).

Conflict of interest: The authors declare no financial or commercial conflict of interest

References

1 **Stavru, F., Archambaud, C. and Cossart, P.,** Cell biology and immunology of *Listeria monocytogenes* infections: novel insights. *Immunol. Rev.* 2011. **240**: 160–184.

2 **Köster, S., Van Pee, K., Hudel, M., Leustik, M., Rhinow, D., Kühlbrandt, W., Chakraborty, T. et al.,** Crystal structure of listeriolysin O reveals molecular details of oligomerization and pore formation. *Nat. Commun.* 2014. **5**: 3690.

3 **Hamon, M., Ribet, D., Stavru, F. and Cossart, P.,** Listeriolysin O: the Swiss army knife of Listeria. *Trends Microbiol.* 2012. **20**: 360–368.

4 **Carrero, J., Vivanco-Cid, H. and Unanue, E.,** Listeriolysin o is strongly immunogenic independently of its cytotoxic activity. *PLoS One* 2012. **7**: 19–32.

5 **Gaillard, J. L., Berche, P. and Sansonetti, P.,** Transposon mutagenesis as a tool to study the role of hemolysin in the virulence of *Listeria monocytogenes*. *Infect. Immun.* 1986. **52**:50–55.

6 **Portnoy, D. A., Jacks, P. S. and Hinrichs, D. J.,** Role of hemolysin for the intracellular growth of *Listeria monocytogenes*. *J. Exp. Med.* 1988. **167**: 1459–1471.

7 **Czuczman, M., Fattouh, R., Van Rijn, J., Canadien, V., Osborne, S., Muise, A., Kuchroo, V. et al.,** *Listeria monocytogenes* exploits efferocytosis to promote cell-to-cell spread. *Nature* 2014. **509**: 230–234.

8 **Gekara, N., Westphal, K., Ma, B., Rohde, M., Groebe, L. and Weiss, S.,** The multiple mechanisms of Ca^{2+} signalling by listeriolysin O, the cholesterol-dependent cytolysin of *Listeria monocytogenes*. *Cell. Microbiol.* 2007. **9**: 2008–2021.

9 **Lam, G., Cemma, M., Muise, A., Higgins, D. and Brumell, J.,** Host and bacterial factors that regulate LC3 recruitment to *Listeria monocytogenes* during the early stages of macrophage infection. *Autophagy* 2013. **9**: 985–995.

10 **Carrero, J., Calderon, B. and Unanue, E.,** Listeriolysin O from *Listeria monocytogenes* is a lymphocyte apoptogenic molecule. *J. Immunol.* 2004. **172**: 4866–4874.

11 **Guzmán, C. A., Domann, E., Rohde, M., Bruder, D., Darji, A., Weiss, S., Wehland, J. et al.,** Apoptosis of mouse dendritic cells is triggered by listeriolysin, the major virulence determinant of Listeria monocytogenes. *Mol. Microbiol.* 1996. **20**: 119–126.

12 **Walter, P. and Ron, D.,** The unfolded protein response: from stress pathway to homeostatic regulation. *Science* 2011. **334**: 1081–1086.

13 **Hetz, C.,** The unfolded protein response: controlling cell fate decisions under ER stress and beyond. *Nat. Rev. Mol. Cell Biol.* 2012. **13**: 89–102.

14 Peña, J. and Harris, E., Dengue virus modulates the unfolded protein response in a time-dependent manner. *J. Biol. Chem.* 2011. **286**: 14226–14236.

15 Merquiol, E., Uzi, D., Mueller, T., Goldenberg, D., Nahmias, Y., Xavier, R., Tirosh, B. et al., HCV causes chronic endoplasmic reticulum stress leading to adaptation and interference with the unfolded protein response. *PLoS One* 2011. **6**: e24660.

16 Tardif, T., Mori, K., Kaufman, R. and Siddiqui, A., Hepatitis C virus suppresses the IRE1-XBP1 pathway of the unfolded protein response. *J. Biol. Chem.* 2004. **279**: 17158–17164.

17 Pavio, N., Romano, P., Graczyk, T., Feinstone, S. and Taylor, D., Protein synthesis and endoplasmic reticulum stress can be modulated by the hepatitis C virus envelope protein E2 through the eukaryotic initiation factor 2 alpha kinase PERK. *J. Virol.* 2003. **77**: 3578–3585.

18 Hassan, I., Zhang, M., Powers, L., Shao, J., Baltrusaitis, J., Rutkowski, D., Legge, K. et al., Influenza A viral replication is blocked by inhibition of the inositol-requiring enzyme 1 (IRE1) stress pathway. *J. Biol. Chem.* 2012. **287**: 4679–4689.

19 Pasqual, G., Burri, D., Pasquato, A., De la Torre, J. and Kunz, S., Role of the host cell's unfolded protein response in arenavirus infection. *J. Virol.* 2011. **85**: 1662–1670.

20 Yamamoto, M., Ma, J., Mueller, C., Kamiyama, S., Saiga, H., Kubo, E., Kimura, T. et al., ATF6beta is a host cellular target of the Toxoplasma gondii virulence factor ROP18. *J. Exp. Med.* 2011. **208**: 1533–1546.

21 Grabiner, M., Fu, Z., Wu, T., Barry, K., Schwarzer, C. and Machen, T., *Pseudomonas aeruginosa* quorum-sensing molecule homoserine lactone modulates inflammatory signaling through PERK and eI-F2a. *J. Immunol.* 2014. **193**: 1459–1467.

22 Seimon, T., Kim, M., Blumenthal, A., Koo, J., Ehrt, S., Wainwright, H., Bekker, L. et al., Induction of ER stress in macrophages of tuberculosis granulomas. *PLoS One* 2010. **5**: e12772.

23 Martinon, F., Chen, X., Lee, A. and Glimcher, L., TLR activation of the transcription factor XBP1 regulates innate immune responses in macrophages. *Nat. Immunol.* 2010. **11**: 411–418.

24 Woo, C., Cui, D., Arellano, J., Dorweiler, B., Harding, H., Fitzgerald, K., Ron, D. et al., Adaptive suppression of the ATF4-CHOP branch of the unfolded protein response by toll-like receptor signalling. *Nat. Cell Biol.* 2009. **11**: 1473–1480.

25 Cho, J., Lee, A., Platzer, B., Cross, B., Gardner, B., De Luca, H., Luong, P. et al., The unfolded protein response element IRE1α senses bacterial proteins invading the ER to activate RIG-I and innate immune signaling. *Cell Host Microbe* 2013. **13**: 558–569.

26 Bettigole, S. and Glimcher, L., Endoplasmic reticulum stress in immunity. *Annu. Rev. Immunol.* 2015. **33**: 107–138.

27 Scheuner, D., Song, B., McEwen, E., Liu, C., Laybutt, R., Gillespie, P., Saunders, T. et al., Translational control is required for the unfolded protein response and in vivo glucose homeostasis. *Mol. Cell* 2001. **7**: 1165–1176.

28 Harding, H., Zhang, Y., Bertolotti, A., Zeng, H. and Ron, D., Perk is essential for translational regulation and cell survival during the unfolded protein response. *Mol. Cell* 2000. **5**: 897–904.

29 Vattem, K. and Wek, R., Reinitiation involving upstream ORFs regulates ATF4 mRNA translation in mammalian cells. *Proc. Natl. Acad. Sci. U. S. A.* 2004. **101**: 11269–11274.

30 Novoa, I., Zeng, H., Harding, H. and Ron, D., Feedback inhibition of the unfolded protein response by GADD34-mediated dephosphorylation of eIF2alpha. *J. Cell Biol.* 2001. **153**: 1011–1022.

31 Dabo, S. and Meurs, E., dsRNA-dependent protein kinase PKR and its role in stress, signaling and HCV infection. *Viruses* 2012. **4**: 2598–2635.

32 Harding, H., Zhang, Y., Zeng, H., Novoa, I., Lu, P., Calfon, M., Sadri, N. et al., An integrated stress response regulates amino acid metabolism and resistance to oxidative stress. *Mol. Cell* 2003. **11**: 619–633.

33 Ishibashi, O., Ali, M. M., Luo, S.-S., Ohba, T., Katabuchi, H., Takeshita, T. and Takizawa, T., Short RNA duplexes elicit RIG-I-mediated apoptosis in a cell type- and length-dependent manner. *Sci. Signal.* 2011. **4**: ra74. DOI: 10.1126/scisignal.2001614.

34 Okumura, F., Okumura, A., Uematsu, K., Hatakeyama, S., Zhang, D. and Kamura, T., Activation of double-stranded RNA-activated protein kinase (PKR) by interferon-stimulated gene 15 (ISG15) modification downregulates protein translation. *J. Biol. Chem.* 2013. **288**: 2839–2847.

35 Carrero, J. and Unanue, E., Mechanisms and immunological effects of apoptosis caused by *Listeria monocytogenes*. *Adv. Immunol.* 2012. **113**: 157–174.

36 Carrero, J., Calderon, B. and Unanue, E., Type I interferon sensitizes lymphocytes to apoptosis and reduces resistance to Listeria infection. *J. Exp. Med.* 2004. **200**: 535–540.

37 O'Connell, R. M., Saha, S. K., Vaidya, S. A., Bruhn, K. W., Miranda, G. A., Zarnegar, B., Perry, A. K. et al., Type I interferon production enhances susceptibility to *Listeria monocytogenes* infection. *J. Exp. Med.* 2004. **200**: 437–445.

38 Auerbuch, V., Brockstedt, D. G., Meyer-Morse, N., O'Riordan, M. and Portnoy, D. A., Mice lacking the type I interferon receptor are resistant to *Listeria monocytogenes*. *J. Exp. Med.* 2004. **200**: 527–533.

39 McCaffrey, R., Fawcett, F., O'Riordan, M., Lee, K., Havell, E., Brown, P. and Portnoy, D., A specific gene expression program triggered by Grampositive bacteria in the cytosol. *Proc. Natl. Acad. Sci. U. S. A.* 2004. **101**: 11386–11391.

40 Stockinger, S., Materna, T., Stoiber, D., Bayr, L., Steinborn, R., Kolbe, T., Unger, H. et al., Production of type I IFN sensitizes macrophages to cell death induced by *Listeria monocytogenes*. *J. Immunol.* 2002. **169**: 6522–6529.

41 Harding, H., Zeng, H., Zhang, Y., Jungries, R., Chung, P., Plesken, H., Sabatini, D. et al., Diabetes mellitus and exocrine pancreatic dysfunction in PERK-/- mice reveals a role for translational control in secretory cell survival. *Mol. Cell* 2001. **7**: 1153–1163.

42 Masuoka, H. C. and Townes, T. M., Targeted disruption of the activating transcription factor 4 gene results in severe fetal anemia in mice. *Blood* 2002. **99**: 736–745.

43 O'Riordan, M., Yi, C., Gonzalez, R., Lee, K. and Portnoy, D., Innate recognition of bacteria by a macrophage cytosolic surveillance pathway. *Proc. Natl. Acad. Sci. U. S. A.* 2002. **99**: 13861–13866.

44 Ingrand, S., Barrier, L., Lafay-Chebassier, C., Fauconneau, B., Page, G. and Hugon, J., The oxindole/imidazole derivative C16 reduces in vivo brain PKR activation. *FEBS Lett.* 2007. **581**: 4473–4478.

45 Farrand, A., LaChapelle, S., Hotze, E., Johnson, A. and Tweten, R., Only two amino acids are essential for cytolytic toxin recognition of cholesterol at the membrane surface. *Proc. Natl. Acad. Sci. U. S. A.* 2010. **107**: 4341–4346.

46 Jammi, N., Whitby, L. and Beal, P., Small molecule inhibitors of the RNA-dependent protein kinase. *Biochem. Biophys. Res. Commun.* 2003. **308**: 50–57.

47 Blalock, W. L., Bavelloni, A., Piazzi, M., Tagliavini, F., Faenza, I., Martelli, A. M., Follo, M. Y. et al., Multiple forms of PKR present in the nuclei of acute leukemia cells represent an active kinase that is responsive to stress. *Leukemia* 2011. **25**: 236–245.

48 **Nakamura, T., Furuhashi, M., Li, P., Cao, H., Tuncman, G., Sonenberg, N., Gorgun, C. Z. et al.**, Double-stranded RNA-dependent protein kinase links pathogen sensing with stress and metabolic homeostasis. *Cell* 2010. **140**: 338–348.

49 **Gusella, G., Musso, T., Rottschafer, S., Pulkki, K. and Varesio, L.**, Potential requirement of a functional double-stranded RNA-dependent protein kinase (PKR) for the tumoricidal activation of macrophages by lipopolysaccharide or IFN-alpha beta, but not IFN-gamma. *J. Immunol.* 1995. **154**: 345–354.

50 **Cullinan, S. and Diehl, A.**, Coordination of ER and oxidative stress signaling: the PERK/Nrf2 signaling pathway. *Int. J. Biochem. Cell Biol.* 2006. **38**: 317–332.

51 **Cullinan, S. and Diehl, J.**, PERK-dependent activation of Nrf2 contributes to redox homeostasis and cell survival following endoplasmic reticulum stress. *J. Biol. Chem.* 2004. **279**: 20108–20117.

52 **Han, J., Back, S., Hur, J., Lin, Y., Gildersleeve, R., Shan, J., Yuan, C. et al.**, ER-stress-induced transcriptional regulation increases protein synthesis leading to cell death. *Nat. Cell Biol.* 2013. **15**: 481–490.

53 **Tabas, I. and Ron, D.**, Integrating the mechanisms of apoptosis induced by endoplasmic reticulum stress. *Nat. Cell Biol.* 2011. **13**: 184–190.

54 **Ferlito, M., Wang, Q., Fulton, W., Colombani, P., Marchionni, L., Fox-Talbot, K., Paolocci, N. et al.**, Hydrogen sulfide [corrected] increases survival during sepsis: protective effect of CHOP inhibition. *J. Immunol.* 2014. **192**: 1806–1814.

55 **Atkins, C., Liu, Q., Minthorn, E., Zhang, S.-Y., Figueroa, D. J., Moss, K., Stanley, T. B. et al.**, Characterization of a novel PERK kinase inhibitor with antitumor and antiangiogenic activity. *Cancer Res.* 2013. **73**: 1993–2002.

56 **Li, G., Mongillo, M., Chin, K., Harding, H., Ron, D., Marks, A. and Tabas, I.**, Role of ERO1-alpha-mediated stimulation of inositol 1,4,5-triphosphate receptor activity in endoplasmic reticulum stress-induced apoptosis. *J. Cell Biol.* 2009. **186**: 783–792.

57 **Endo, M., Mori, M., Akira, S. and Gotoh, T.**, C/EBP homologous protein (CHOP) is crucial for the induction of caspase-11 and the pathogenesis of lipopolysaccharide-induced inflammation. *J. Immunol.* 2006. **176**: 6245–6253.

58 **Allagnat, F., Fukaya, M., Nogueira, T., Delaroche, D., Welsh, N., Marselli, L., Marchetti, P. et al.**, C/EBP homologous protein contributes to cytokine-induced pro-inflammatory responses and apoptosis in β-cells. *Cell Death Differ.* 2012. **19**: 1836–1846.

59 **Oyadomari, S. and Mori, M.**, Roles of CHOP/GADD153 in endoplasmic reticulum stress. *Cell Death Differ.* 2004. **11**: 381–389.

60 **Hiramatsu, N., Chiang, W., Kurt, T., Sigurdson, C. and Lin, J.**, Multiple mechanisms of unfolded protein response-induced cell death. *Am. J. Pathol.* 2015. **185**: 1800–1808.

61 **Sauer, J., Witte, C., Zemansky, J., Hanson, B., Lauer, P. and Portnoy, D.**, Listeria monocytogenes triggers AIM2-mediated pyroptosis upon infrequent bacteriolysis in the macrophage cytosol. *Cell Host Microbe* 2010. **7**: 412–409.

62 **Zinszner, H., Kuroda, M., Batchvarova, N., Lightfoot, R., Remotti, H., Stevens, J. and Ron, D.**, CHOP is implicated in programmed cell death in response to impaired function of the endoplasmic reticulum. *Genes Dev.* 1998. **12**: 982–995.

63 **Inaba, K., Inaba, M., Romani, N., Aya, H., Deguchi, M., Ikehara, S., Muramatsu, S. et al.**, Generation of large numbers of dendritic cells from mouse bone marrow cultures supplemented with granulo-cyte/macrophage colony-stimulating factor. *J. Exp. Med.* 1992. **176**: 1693–1702.

64 **Celada, A., Gray, P., Rinderknecht, E. and Schreiber, R.**, Evidence for a gamma-interferon receptor that regulates macrophage tumoricidal activity. *J. Exp. Med.* 1984. **160**: 55–74.

65 **Edelson, B., Bradstreet, T., Hildner, K., Carrero, J., Frederick, K., KC, W., Belizaire, R. et al.**, CD8α(+) dendritic cells are an obligate cellular entry point for productive infection by Listeria monocytogenes. *Immunity* 2011. **35**: 236–248.

66 **Stockinger, S., Kastner, R., Kernbauer, E., Pilz, A., Westermayer, S., Reutterer, B., Soulat, D. et al.**, Characterization of the interferon-producing cell in mice infected with *Listeria monocytogenes*. *PLoS Pathog.* 2009. **5**: e1000355.

67 **Allen, J. R., Nguyen, L. X., Sargent, K. E. G., Lipson, K. L., Hackett, A. and Urano, F.**, High ER stress in beta-cells stimulates intracellular degradation of misfolded insulin. *Biochem. Biophys. Res. Commun.* 2004. **324**: 166–170.

68 **Wheeler, M., Rizzi, M., Sasik, R., Almanza, G., Hardiman, G. and Zanetti, M.**, KDEL-retained antigen in B lymphocytes induces a proinflammatory response: a possible role for endoplasmic reticulum stress in adaptive T cell immunity. *J. Immunol.* 2008. **181**: 256–264.

69 **Kozutsumi, Y., Segal, M., Normington, K., Gething, M. J. and Sambrook, J.**, The presence of malfolded proteins in the endoplasmic reticulum signals the induction of glucose-regulated proteins. *Nature* 1988. **332**: 462–464.

70 **Fonseca, S. G., Fukuma, M., Lipson, K. L., Nguyen, L. X., Allen, J. R., Oka, Y. and Urano, F.**, WFS1 is a novel component of the unfolded protein response and maintains homeostasis of the endoplasmic reticulum in pancreatic beta-cells. *J. Biol. Chem.* 2005. **280**: 39609–39615.

71 **Calfon, M., Zeng, H., Urano, F., Till, J. H., Hubbard, S. R., Harding, H. P., Clark, S. G. et al.**, IRE1 couples endoplasmic reticulum load to secretory capacity by processing the XBP-1 mRNA. *Nature* 2002. **415**: 92–96.

72 **Glomski, I., Gedde, M., Tsang, A., Swanson, J. and Portnoy, D.**, The Listeria monocytogenes hemolysin has an acidic pH optimum to compartmentalize activity and prevent damage to infected host cells. *J. Cell Biol.* 2002. **156**: 1029–1038.

Full correspondence: Dr. Javier A. Carrero, Washington University School of Medicine, 660 S. Euclid Avenue, St. Louis, MO 63110, USA
e-mail: jacarrer@wustl.edu